Consciousness and Cognition 58 (2018) 158–169

Contents lists available at ScienceDirect

Consciousness and Cognition

journal homepage: www.elsevier.com/locate/concog

Emotional prediction: An ALE meta-analysis and MACM analysis

Guangming Ran[a,*], Xiaojun Cao[a], Xu Chen[b]

[a] Department of Psychology, Institute of Education, China West Normal University, Nanchong 637002, China
[b] Faculty of Psychology, Southwest University, Chongqing 400715, China

ARTICLE INFO

Keywords:
Emotional prediction
Dorsolateral prefrontal cortex
Ventrolateral prefrontal cortex
Orbitofrontal cortex
ALE
MACM

ABSTRACT

The prediction of emotion has been explored in a variety of functional brain imaging and neurophysiological studies. However, an overall picture of the areas involved this process remains unexploited. Here, we quantitatively summarized the published literature on emotional prediction using activation likelihood estimation (ALE) in functional magnetic resonance imaging (fMRI). Furthermore, the current study employed a meta-analytic connectivity modeling (MACM) to map the meta-analytic coactivation maps of regions of interest (ROIs). Our ALE analysis revealed significant convergent activations in some vital brain areas involved in emotional prediction, including the dorsolateral prefrontal cortex (DLPFC), ventrolateral prefrontal cortex (VLPFC), orbitofrontal cortex (OFC) and medial prefrontal cortex (MPFC). For the MACM analysis, we identified that the DLPFC, VLPFC and OFC were the core areas in the coactivation network of emotional prediction. Overall, the results of ALE and MACM indicated that prefrontal brain areas play critical roles in emotional prediction.

1. Introduction

Human beings live in an uncertain world, which leads to a huge loss, and ultimately affects their physical and mental health. Humans, however, do not process external environment stimuli passively, but continuously generate top-down predictions about them (Kveraga, Ghuman, & Bar, 2007). Pre-awareness of emotional information conveyed by others enables individuals to act appropriately in social exchanges (Lin et al., 2012; Peng, De, Yuan, & Zhou, 2012; Ran, Chen, Pan, Hu, & Ma, 2014).

An increasing number of studies have explored the neural underpinnings underlying emotional prediction. For example, Nitschke, Sarinopoulos, Mackiewicz, Schaefer, and Davidson (2006) have demonstrated that the prediction of a negative emotional stimulus triggers brain areas involved in the experience of negative emotion. This find is consistent with the functional magnetic resonance imaging (fMRI) result that predictable unpleasant stimuli relative to predictable neutral stimuli result in activation of mainly anterior insula, striatum, thalamus, hypothalamus, amygdala, cingulate cortex and prefrontal areas (Herwig, Abler, Walter, & Erk, 2007). While some reports have observed enhanced neural responses in supracallosal anterior cingulated cortex, ventrolateral prefrontal cortex, insula, and amygdala for predictable emotional events (both positive and negative) compared to unpredictable ones (e.g. Onoda et al., 2008), several other studies reported a reversed pattern of activation in insula and amygdala for predictable negative emotional stimuli compared with unpredictable ones (e.g. Sarinopoulos et al., 2010). Such discrepancies may arise from differences in experimental task and stimuli. For instance, in the study of Onoda et al. (2008), participants were instructed to detect an auditory cue. However, a visual cue was employed in the study of Sarinopoulos et al. (2010).

Our recent study have showed decreased activity in the right dorsolateral prefrontal cortex for predictable fear faces and increased activity in the left for predictable happy faces, suggesting that positive and negative emotional prediction may be two distinct

* Corresponding author.
E-mail address: haiqi49@cwnu.edu.cn (G. Ran).

http://dx.doi.org/10.1016/j.concog.2017.10.019
Received 26 September 2017; Received in revised form 21 October 2017; Accepted 30 October 2017
Available online 08 November 2017
1053-8100/

processes (Ran, Chen, Zhang, Ma, & Zhang, 2016a). There has been a growing recognition that altered prediction of future negative emotional events may be a key aspect of anxiety disorders (Eysenck, 1997; Grillon, 2008). For example, evidence from functional MRI data suggests that brain activation on the right insula is significantly higher in high trait anxiety compared to anxiety normative individuals during aversive prediction (Simmons et al., 2011). Moreover, it is found that heightened anxiety in generalized anxiety patients is associated with increased activation in middle frontal areas and the insula when they anticipate encountering negative emotional stimuli (Schlund, Verduzco, Cataldo, & Hoehnsaric, 2012). More recently, some researchers have reported that greater activation in the bilateral anterior insula was observed in posttraumatic stress disorder (PTSD) versus control subjects during prediction of unpleasant (combat-related) images (Aupperle et al., 2012; Simmons et al., 2013).

Although a wealth of research has investigated the neural correlates of emotional prediction, an overall picture of the areas involved this process remains unexploited. Therefore, the present study adopted a meta-analysis approach of brain imaging studies to identify human brain areas associated with emotional prediction. We adopted an activation likelihood estimation (ALE) meta-analysis because it can accommodate the large amounts of data generated across multiple studies (Eickhoff et al., 2009; Eysenck, 1997; Laird et al., 2005). In addition, a meta-analytic connectivity modeling (MACM) was employed to analyse the co-occurring network of emotional prediction (Eickhoff et al., 2011; Laird et al., 2013; Robinson, Laird, Glahn, Lovallo, & Fox, 2010).

2. Materials and methods

2.1. Literature search and selection

Relevant studies were identified through a systematic online database search for peer-reviewed articles published before October 2016 on PubMed Database, ISI Web of Knowledge and Google Scholar. Searches were conducted with the keywords “fMRI” or “positron emission tomography (PET)”, in combination with one or two of the following search terms: “prediction”, “anticipation”, “expectation”, “inference”, “foresight”, “prospection”, “forecasting”, “preparation”, “emotion”, “expression”, “happy faces”, “aversive pictures”, “negative emotion”, “positive emotion”, “angry faces” and “fear faces”.

The search yielded 36 potential studies that were further assessed according to the following requirements: (1) the subjects in the selected studies were healthy individuals; (2) the coordinates in the studies were in Talairach or in Montral Neurological Institute (MNI) space; (3) the studies applied whole-brain general-linear-model-based analyses. A total of 18 imaging studies were included in the final meta-analysis (Table 1). These studies included six experimental contrasts: Predictable > Unpredictable, Unpredictable > Predictable, Predictable negative > Unpredictable negative, Predictable positive > Unpredictable positive, Unpredictable negative > Predictable negative, Unpredictable positive > Predictable positive. Some studies contributed more than one experimental contrast. For example, the study of Ueda et al. (2003) included two experimental contrasts.

2.2. Activation likelihood estimation meta-analysis approach

An activation likelihood estimation (ALE) meta-analysis (Eickhoff et al., 2009) was conducted using the GingerALE software (version 2.3, http://www.brainmap.org/ale/). Applying the ALE analysis, the reported coordinates of brain areas involving in emotional prediction were converged across different experiments. Give that various emotional predictions might activate different brain areas, we converged the coordinates of the areas associating with negative (angry, fearful and aversive) and positive (happy) emotional prediction. To determine statistical significance, we run a permutation test of randomly distributed foci with 5000 simulations (Feng, Luo, & Krueger, 2015). The ALE-maps had a threshold at a false discovery rate (FDR) of $p < 0.05$

Table 1
All studies entered into the meta analysis are listed, including year, first author, neuroimaging, number of subjects and experimental contrast.

Year	First author	Neuroimaging	Number of subjects	Experimental contrast
2003	Ueda	fMRI	15	Predictable negative > Unpredictable negative, Predictable positive > Unpredictable positive
2004	Simmons	fMRI	28	Unpredictable > Predictable
2006	Bermpohl	fMRI	17	Predictable positive > Unpredictable positive
2006	Simmons	fMRI	32	Unpredictable > Predictable
2007a	Herwig	fMRI	12	Unpredictable > Predictable
2007b	Herwig	fMRI	34	Unpredictable > Predictable
2007c	Herwig	fMRI	16	Predictable > Unpredictable
2008	Onoda	fMRI	18	Predictable > Unpredictable
2010	Schienle	fMRI	30	Unpredictable negative > Predictable negative
2010	Sarinopoulos	fMRI	40	Unpredictable negative > Predictable negative
2011	Clauss	fMRI	42	Predictable > Unpredictable
2011	Brühl	fMRI	14	Unpredictable > Predictable
2012	Barbalat	fMRI	26	Unpredictable negative > Predictable negative
2014	Lutz	fMRI	46	Unpredictable > Predictable
2014	Greenberg	fMRI	25	Unpredictable > Predictable
2016	Ran_EXP 1	fMRI	24	Predictable negative > Unpredictable negative, Unpredictable negative > Predictable negative
2016	Ran_EXP 2	fMRI	25	Predictable positive > Unpredictable positive, Unpredictable positive > Predictable positive
2016	Dzafic	fMRI	28	Predictable > Unpredictable; Unpredictable > Predictable

(Cromheeke & Mueller, 2014) and a minimum cluster size of $k > 50\,mm^3$ (Palermo, Benedetti, Costa, & Amanzio, 2015).

2.3. Meta-analytic connectivity modeling

Given that prefrontal cortices (e.g., DLPFC, VLPFC and OFC) play critical roles in emotional prediction (Herwig, Kaffenberger, Baumgartner, & Jäncke, 2007; Herwig et al., 2007; Onoda et al., 2008), a meta-analytic connectivity modeling (MACM) was used to assess bilateral DLPFC, VLPFC and OFC separately. These prefrontal cortex ROIs were defined by the Wake Forest University School of Medicine (WFU) PickAtlas. All ROIs were input into the BrainMap database to search for the studies that reported activation within each ROI boundary (Robinson et al., 2010). The present study included the experiment-level search criteria of "context: normal mapping" and "activations: activation only".

We then downloaded whole-brain coordinates of activations from identified contrasts (left DLPFC = 21,788 total number of subjects, 1454 number of experiments, 32,736 number of foci; right DLPFC = 18,255 total number of subjects, 1205 number of experiments, 26,931 number of foci; left VLPFC = 16,746 total number of subjects, 1104 number of experiments, 23,433 number of foci; right VLPFC = 14,206 total number of subjects, 943 number of experiments, 20,847 number of foci; left OFC = 4714 total number of subjects, 313 number of experiments, 6106 number of foci; right OFC = 5229 total number of subjects, 360 number of experiments, 7256 number of foci). To determine brain areas of convergence, the foci resulting from each ROI search were analysed using the ALE meta-analysis.

3. Results

3.1. Meta-analysis

3.1.1. Emotional prediction

The ALE analysis revealed that unpredictable stimuli evoked greater likelihood of activation than predictable stimuli in the left insula and right anterior cingulate cortex. Conversely, predictable stimuli triggered increased likelihood of activation compared to unpredictable stimuli in an extensive brain areas, including the right ventrolateral prefrontal cortex (VLPFC), right orbitofrontal cortex (OFC), left dorsolateral prefrontal cortex (DLPFC), right medial prefrontal cortex (MPFC), left pre-motor cortex (PMC), bilateral middle occipital gyrus (MOG), bilateral amygdala, left anterior cingulate cortex (ACC), right lingual gyrus, right parahippocampal gyrus and right cerebellum (Table 2 and Fig. 1A and B).

3.1.2. Negative and positive emotional prediction

The analysis showed that unpredictable negative emotional stimuli produced greater activation than predictable negative emotional stimuli in the bilateral insula and left amygdala. No other suprathreshold activation was found at current analysis (Table 2 and Fig. 1C).

Table 2
Areas of activations resulting from the meta-analysis of emotional prediction.

Cluster #	Volume (mm^3)	Brain areas	BA	Side	Extrema value	MNI coordinates		
						X	Y	Z
Unpredictable > Predictable								
1	224	Insula		L	0.02075536	−32	24	2
2	64	Anterior cingulate cortex	47	R	0.01878892	6	12	2
Predictable > Unpredictable								
1	192	Ventrolateral prefrontal cortex	47	R	0.01625913	30	22	−10
2	184	Amygdala		L	0.01682575	−24	0	−20
3	160	Parahippocampal gyrus	36	R	0.01628199	28	−4	−28
4	160	Amygdala		R	0.01573155	30	−6	−14
5	96	Cerebellum		R	0.01448945	16	−82	−38
6	96	Anterior cingulate cortex	32	R	0.01470698	−8	42	6
7	96	Middle occipital gyrus	19	R	0.01448939	38	−65	9
8	96	Orbitofrontal cortex	10	R	0.01525332	10	66	20
9	80	Middle occipital gyrus	19	L	0.01493956	−38	−75	6
10	80	Lingual gyrus	17	R	0.01499071	12	−84	8
11	80	Dorsolateral prefrontal cortex	9	L	0.01493958	−42	8	36
12	64	Medial prefrontal cortex	10	R	0.01412205	2	54	12
13	56	Pre-motor cortex	6	L	0.01542439	−10	20	50
Negative unpredictable > Negative predictable								
1	240	Insula	13	L	0.01583033	−34	24	4
2	216	Insula	13	R	0.0147316	34	20	4
3	176	Amygdala		L	0.01344163	−18	−10	−16

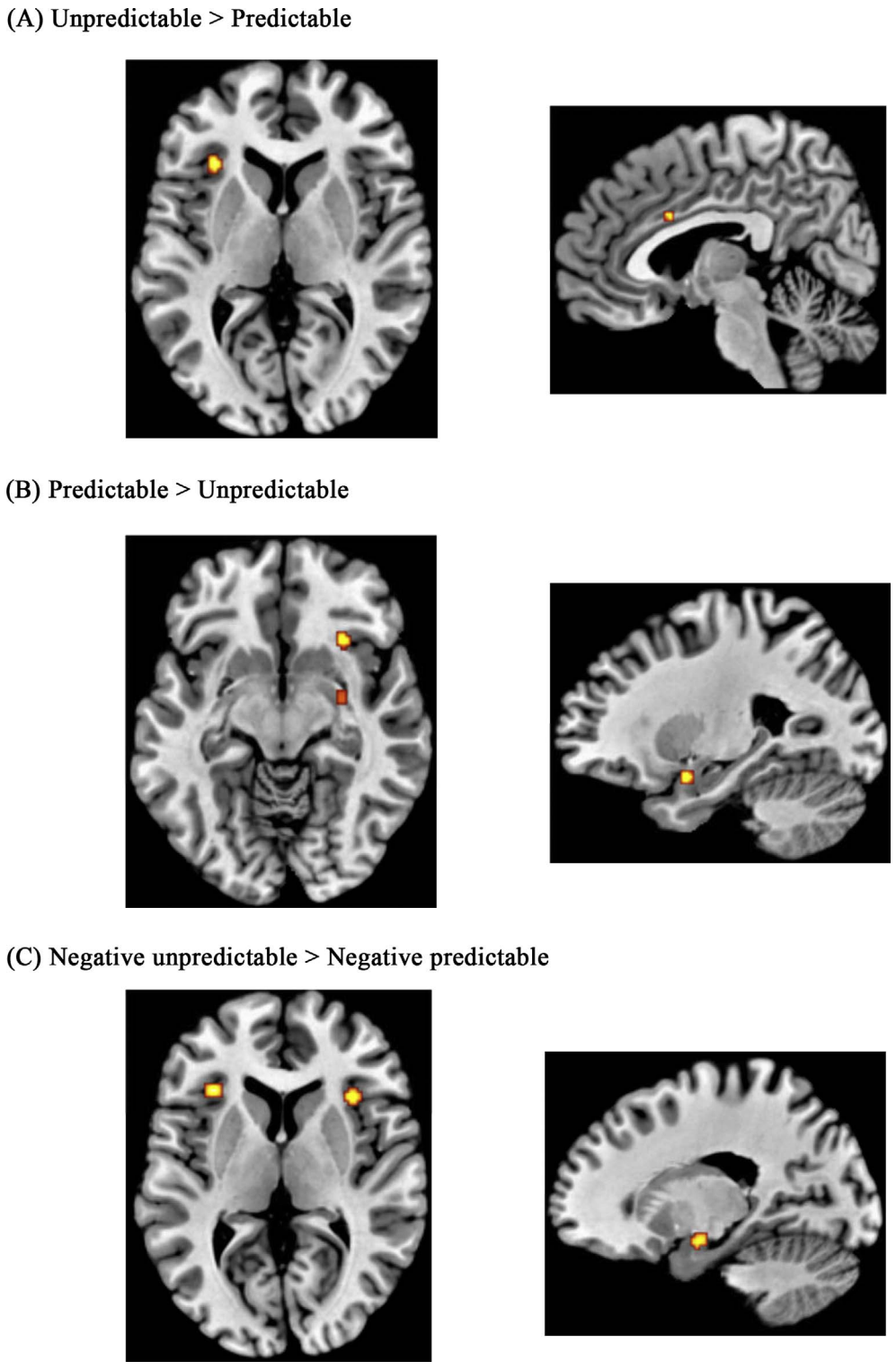

Fig. 1. Displayed are significant results from the meta-analysis of emotional prediction (FDR corrected < 0.05).

3.2. MACM analysis

MACM maps for the six selected seed ROIs (bilateral DLPFC, VLPFC and OFC) were computed by an ALE meta-analysis of those experiments in the BrainMap that featured the closest activation foci to each seed ROI.

Table 3
MACM results: areas of functional coactivation associated with left DLPFC.

Cluster #	Volume (mm^3)	Brain areas	BA	Side	Extrema value	MNI coordinates		
						X	Y	Z
1	266,072	Inferior frontal gyrus	9	L	0.7362504	−44	6	32
		Inferior frontal gyrus	9	R	0.5230269	44	6	32
		Superior frontal gyrus	6	L	0.6335599	−4	10	48
		Middle frontal gyrus	6	L	0.6081479	−28	6	52
		Middle frontal gyrus	6	R	0.4129703	26	−6	52
		Insula	13	L	0.5757914	−32	20	6
		Insula	13	R	0.5719996	32	20	4
		Inferior parietal lobule	40	L	0.5142001	−32	−54	44
		Inferior parietal lobule	7	R	0.4482162	32	−56	44
		Superior parietal lobule	7	L	0.5073428	−28	−62	42
		Thalamus		L	0.3983115	−12	−16	8
		Thalamus		R	0.3397772	8	−16	10
		Fusiform gyrus	37	L	0.3318906	−42	−58	−12
		Middle temporal gyrus	22	L	0.3191858	−54	−40	2
		Caudate		R	0.3156643	14	4	8
		Lentiform nucleus		L	0.3044687	−18	2	6
		Precuneus	31	R	0.2549571	28	−72	28
		Inferior occipital gyrus	18	L	0.218121	−26	−88	−4
		Superior temporal gyrus	39	L	0.215422	−48	−58	20
		Anterior lobe		L	0.2137947	−32	−54	−28
		Middle occipital gyrus	18	L	0.2080504	−30	−82	4
		Postcentral gyrus	40	L	0.2008179	−54	−26	18
2	7744	Culmen		R	0.2718238	30	−60	−24
		Middle frontal gyrus	18	R	0.2563028	28	−84	0
		Fusiform gyrus	37	R	0.2229782	40	−52	−16
		Inferior temporal gyrus	37	R	0.2228067	−44	−66	−2
		Inferior occipital gyrus	37	L	0.2183445	−36	−78	−4
3	1736	Superior temporal gyrus	22	R	0.2091097	50	−32	4

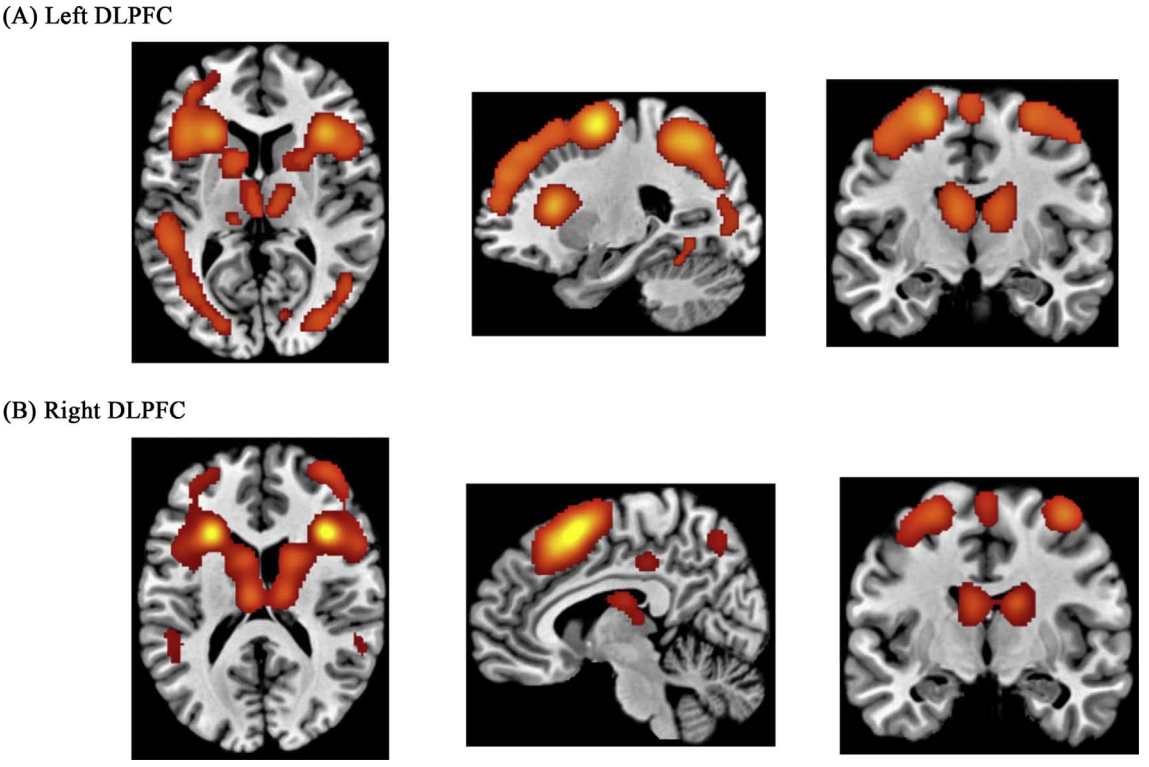

Fig. 2. Depicted are connectivity maps corrected for multiple comparisons (FDR corrected < 0.001) for the left DLPFC (A) and right DLPFC (B).

Table 4
MACM results: areas of functional coactivation associated with right DLPFC.

Cluster #	Volume (mm^3)	Brain areas	BA	Side	Extrema value	MNI coordinates		
						X	Y	Z
1	186,024	Insula	13	R	0.58110505	32	20	4
		Insula	13	L	0.53685397	−32	18	6
		Middle frontal gyrus	6	R	0.57003415	32	−4	52
		Middle frontal gyrus	6	L	0.41123897	−28	−6	54
		Superior frontal gyrus	6	L	0.5633013	0	10	48
		Inferior frontal gyrus	9	L	0.50561464	−44	6	30
		Thalamus		L	0.34930396	−12	−18	10
		Thalamus		R	0.3455567	8	−16	10
		Lentiform nucleus		R	0.32357493	14	4	6
		Lentiform nucleus		L	0.31550246	−14	2	10
2	58,800	Inferior parietal lobule	7	R	0.42948908	32	−56	44
		Inferior parietal lobule	40	L	0.4261198	−34	−52	42
		Superior parietal lobule	7	L	0.3973839	−28	−62	44
		Middle occipital gyrus	19	L	0.20509864	−28	−80	18
		Superior temporal gyrus	13	R	0.20483033	54	−42	16
		Middle temporal gyrus	22	R	0.18184929	54	−46	0
3	7176	Fusiform gyrus	37	L	0.25494716	−44	−64	−10
		Inferior occipital gyrus	18	L	0.16862163	−28	−86	−6
4	3192	Culmen		R	0.20973906	30	−58	−26
		Middle temporal gyrus	37	R	0.19234005	46	−62	−2
		Fusiform gyrus	37	R	0.1909914	44	−54	−12
5	1816	Middle temporal gyrus	21	L	0.20114096	−52	−42	8
6	1224	Cingulate gyrus	31	L	0.24060914	0	−30	30

The left DLPFC showed higher coactivation probabilities in the inferior/middle and superior frontal gyrus, insula, inferior and superior parietal lobule, fusiform gyrus, inferior/middle and superior temporal gyrus, caudate, thalamus, lentiform nucleus, precuneus, inferior/middle occipital gyrus, anterior lobe, postcentral gyrus, and culmen (Table 3 and Fig. 2A). The right DLPFC demonstrated significantly higher coactivation probabilities in the insula, inferior/middle and superior/medial frontal gyrus, thalamus, lentiform nucleus, inferior and superior parietal lobule, inferior/middle occipital gyrus, inferior and superior temporal gyrus, fusiform gyrus, cingulate gyrus, and culmen (Table 4 and Fig. 2B).

Co-activation maps for the left VLPFC were significant for the insula, inferior/middle and superior/medial frontal gyrus, thalamus, precentral gyrus, middle and superior temporal gyrus, inferior and superior parietal lobule, fusiform gyrus, putamen, amygdala, culmen, middle occipital gyrus, postcentral gyrus, and midbrain (Table 5 and Fig. 3A). Co-activation maps for the right VLPFC included the insula, inferior/middle and superior/medial frontal gyrus, thalamus, postcentral gyrus, putamen, amygdala, caudate body, inferior and superior parietal lobule, middle/superior and transverse/inferior temporal gyrus, inferior/middle occipital gyrus, culmen, precuneus, fusiform gyrus, and sub-gyral (Table 6 and Fig. 3B).

The analysis for the left OFC revealed convergent co-activation in the sub-gyral, inferior/middle and superior/medial frontal gyrus, insula, cingulate gyrus, inferior and superior parietal lobule, middle temporal gyrus, superior occipital gyrus, and precuneus (Table 7 and Fig. 4A). Significant co-activation for the right OFC was observed in the sub-gyral, inferior/middle and superior frontal gyrus, insula, cingulate gyrus, inferior and superior parietal lobule, claustrum, thalamus, fusiform gyrus, and precuneus (Table 8 and Fig. 4B).

4. Discussion

The present work employed a meta-analytic approach to identify brain areas that were consistently implicated in emotional prediction. The ALE analysis revealed significant convergent activations in several brain areas, and these areas were proposed to play an important role in prediction processing. For the MACM analysis, we found that prefrontal areas (e.g., bilateral DLPFC, VLPFC and OFC) showed higher coactivation probabilities in cortical and subcortical areas.

4.1. Brain areas involved emotional prediction

The ALE analysis revealed that predictable emotional stimuli triggered increased likelihood of activation compared to unpredictable emotional stimuli in the prefrontal cortices, left pre-motor cortex, bilateral middle occipital gyrus, bilateral amygdala, left anterior cingulate cortex and right parahippocampal gyrus. This seems to suggest a widespread network of brain areas involved in enhanced effect of emotional prediction, which fits well with the findings of a recent high-quality meta-analysis on pain anticipation (Palermo et al., 2015).

Table 5
MACM results: areas of functional coactivation associated with left VLPFC.

Cluster #	Volume (mm^3)	Brain areas	BA	Side	Extrema value	MNI coordinates		
						X	Y	Z
1	197,136	Insula	13	L	0.6749499	−36	18	6
		Insula	13	R	0.47968704	34	20	2
		Inferior frontal gyrus	47	L	0.6725276	−44	18	2
		Inferior frontal gyrus	9	R	0.36848822	44	6	30
		Precentral gyrus	6	L	0.39513284	−44	−4	46
		Thalamus		L	0.3916901	−10	−16	8
		Thalamus		R	0.30070382	8	−16	8
		Middle temporal gyrus	22	L	0.3716288	−54	−38	2
		Superior parietal lobule	7	L	0.32423133	−30	−58	42
		Fusiform gyrus	37	L	0.29816908	−42	−52	−16
		Putamen		L	0.29676867	−16	6	8
		Putamen		R	0.28560817	−16	4	8
		Middle frontal gyrus	46	R	0.28767124	46	22	24
		Middle frontal gyrus	10	L	0.27436322	−34	44	20
		Inferior parietal lobule	40	L	0.2795156	−38	−46	40
		Superior temporal gyrus	22	R	0.24861999	50	−32	4
		Superior temporal gyrus	41	L	0.214241	−54	−22	6
		Amygdala		L	0.24423444	−20	−8	−10
		Amygdala		R	0.19323738	22	−4	−12
		Culmen		L	0.18969026	−28	−54	−24
		Postcentral gyrus	40	L	0.18127061	−54	−24	22
		Midbrain	40	L	0.17406552	−6	−22	−8
		Middle occipital gyrus	18	L	0.17403851	−40	−76	−8
2	27,736	Superior frontal gyrus	6	L	0.52941054	−4	6	52
		Medial frontal gyrus	6	L	0.52557033	−2	12	46
3	6416	Inferior parietal lobule	7	R	0.28489482	32	−56	42
4	3792	Culmen		R	0.22085397	28	−58	−24

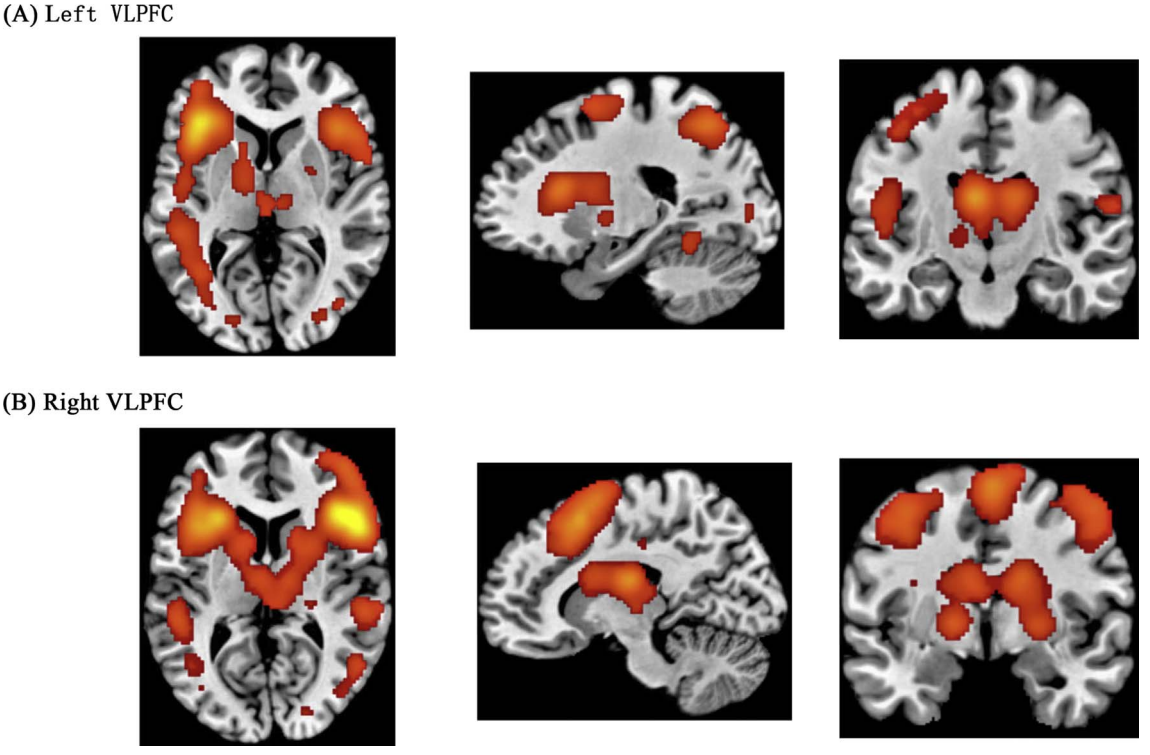

Fig. 3. Depicted are connectivity maps corrected for multiple comparisons (FDR corrected < 0.001) for the left VLPFC (A) and right VLPFC (B).

Table 6
MACM results: areas of functional coactivation associated with right VLPFC.

Cluster #	Volume (mm^3)	Brain areas	BA	Side	Extrema value	MNI coordinates		
						X	Y	Z
1	142,192	Insula	13	R	0.6321964	30	20	4
		Insula	13	L	0.5617772	−32	18	6
		Inferior frontal gyrus	9	R	0.5109156	48	14	22
		Inferior frontal gyrus	9	L	0.3805479	−46	8	26
		Thalamus		L	0.3751861	−12	−18	10
		Thalamus		R	0.3511351	8	−16	8
		Precentral gyrus	44	L	0.3207494	−50	10	8
		Middle frontal gyrus	46	R	0.3136648	46	30	14
		Middle frontal gyrus	10	L	0.2057541	−38	46	14
		Putamen		R	0.2765254	18	2	6
		Amygdala		L	0.2533121	−20	−6	−10
		Amygdala		R	0.2332257	20	−6	−10
		Caudate body		L	0.2474052	−14	0	12
		Putamen		L	0.2403848	−20	6	4
		Superior frontal gyrus	9	L	0.1922936	−36	34	30
		Sub-gyral	6	L	0.1532323	−28	0	52
2	5824	Medial frontal gyrus	6	R	0.4500386	2	12	46
		Superior frontal gyrus	6	L	0.4382779	0	4	52
3	25,760	Inferior parietal lobule	40	L	0.3378664	−32	−52	42
		Middle temporal gyrus	22	L	0.2746228	−52	−44	4
		Postcentral gyrus	40	L	0.1735503	−54	−24	20
		Transverse temporal gyrus	41	L	0.1706013	−56	−22	10
4	21,208	Inferior parietal lobule	40	R	0.2655307	42	−46	42
		Middle temporal gyrus	21	R	0.2484367	50	−32	2
		Superior parietal lobule	7	R	0.2467424	42	−46	42
		Superior temporal gyrus	13	R	0.2001007	56	−44	18
		Postcentral gyrus	40	R	0.1743573	54	−28	20
		Precuneus	31	R	0.1444479	28	−70	28
5	9456	Fusiform gyrus	37	L	0.2693448	−40	−56	−16
		Middle occipital gyrus	37	L	0.2193942	−46	−62	−8
6	5808	Fusiform gyrus	37	R	0.1991116	38	−48	−16
		Inferior temporal gyrus	37	R	0.1944656	46	−64	−2
		Inferior occipital gyrus	19	R	0.1726533	38	−76	−6
		Culmen		R	0.1458598	28	−56	−24

Table 7
MACM results: areas of functional coactivation associated with left OFC.

Cluster #	Volume (mm^3)	Brain areas	BA	Side	Extrema value	MNI coordinates		
						X	Y	Z
1	51,736	Sub-gyral	6	L	0.24147032	−24	4	56
		Superior frontal gyrus	8	L	0.15403268	−20	28	48
		Inferior frontal gyrus	9	L	0.11701537	−48	6	28
		Insula	13	L	0.11280715	−34	22	4
		Middle frontal gyrus	46	L	0.10988657	−44	18	20
		Cingulate gyrus	32	R	0.10539477	2	20	42
		Medial frontal gyrus	9	L	0.08147435	−4	50	18
2	11,024	Superior parietal lobule	7	L	0.12112684	−26	−64	44
		Inferior parietal lobule	7	L	0.11147733	−32	−56	42
		Middle temporal gyrus	39	L	0.09823898	−48	−68	18
		Superior occipital gyrus	19	L	0.08747105	−38	−76	24
		Precuneus	7	L	0.0872701	−10	−72	48
3	1936	Insula	13	R	0.13413933	32	18	2
4	1936	Inferior parietal lobule	40	R	0.09681629	38	−42	46
		Superior parietal lobule	7	R	0.08647623	32	−54	44
5	1448	Precuneus	31	L	0.08831251	−6	−46	30
6	1192	Sub-gyral	6	R	0.1007524	24	0	54

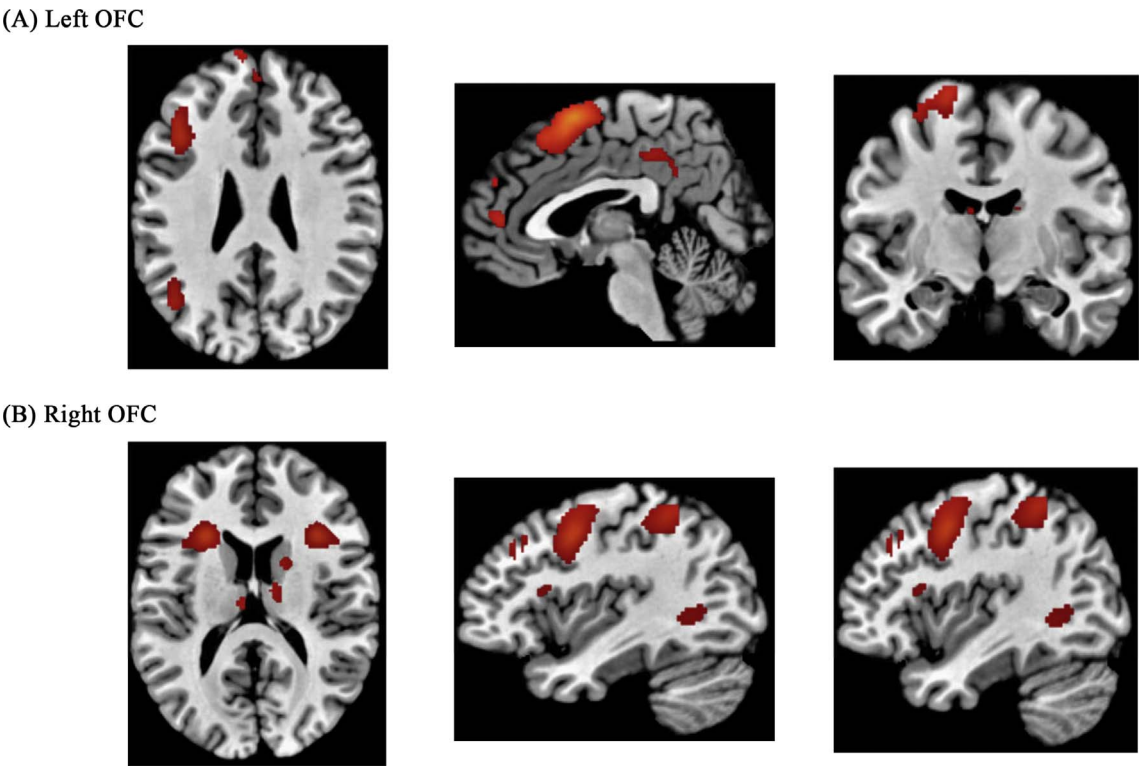

Fig. 4. Depicted are connectivity maps corrected for multiple comparisons (FDR corrected < 0.001) for the left OFC (A) and right OFC (B).

Table 8
MACM results: areas of functional coactivation associated with right OFC.

Cluster #	Volume (mm^3)	Brain areas	BA	Side	Extrema value	MNI coordinates		
						X	Y	Z
1	61,640	Sub-gyral	6	R	0.428281	24	−6	54
		Middle frontal gyrus	6	L	0.23787703	−26	−8	54
		Middle frontal gyrus	9	R	0.13416733	38	30	34
		Superior frontal gyrus	6	L	0.2212773	0	4	52
		Superior frontal gyrus	8	R	0.1391137	24	22	48
		Inferior frontal gyrus	6	L	0.1708107	−46	2	32
		Inferior frontal gyrus	9	R	0.16895764	46	4	28
		Cingulate gyrus	32	R	0.1381881	2	16	38
		Cingulate gyrus	4	L	0.08852809	−36	−20	52
2	7008	Inferior parietal lobule	40	R	0.15114327	36	−44	44
		Superior parietal lobule	7	R	0.13544479	30	−58	44
		Precuneus	19	R	0.10212202	30	−72	28
3	4664	Precuneus	7	L	0.1408704	−20	−66	50
4	4104	Claustrum		R	0.17027555	30	18	6
5	3608	Insula	13	L	0.18245731	−30	18	8
6	2984	Precuneus	7	R	0.14191538	16	−66	50
7	1800	Inferior parietal lobule	40	L	0.15114327	−38	−48	40
8	1256	Superior parietal lobule	7	R	0.13940944	28	−60	44
		Precuneus	31	R	0.11181261	28	−72	28
9	1192	Thalamus		R	0.10587945	8	−18	10
10	1192	Superior parietal lobule	7	R	0.13900226	26	−60	44
		Precuneus	19	R	0.10806714	26	−72	30
11	1096	Caudate		R	0.11064083	14	4	8
12	1032	Superior parietal lobule	7	R	0.13435224	24	−64	48
		Precuneus	7	R	0.09368543	24	−72	30
13	1024	Fusiform gyrus	37	L	0.0941305	−44	−56	−10
14	1008	Thalamus		L	0.10490095	−12	−20	10

A reversed pattern of results was observed in the left insula and right anterior cingulate cortex. This silencing effect of emotional prediction is consistent with previous studies observing reduced neural responses (e.g. Chen, Ran, Zhang, & Hu, 2015) and in line with theoretical models of prediction (Friston, 2005; Friston, 2009). The predictive coding theories propose that a large prediction error will not ensue when the sensory inputs match the observer's predictions, leading to a decrease in neural activity (Kok, Jehee, & de Lange, 2012).

It has previously been argued that the amygdala is thought to play a critical role in negative emotion processing (Hamann & Kilts, 2002; Lanteaume et al., 2007). Our further analysis showed that unpredictable negative emotional stimuli produced greater activation than predictable negative emotional stimuli in the left amygdala, implying that unpredictability about potential negative emotional stimuli may amplify the negative impact of them. This viewpoint is supported by our recent functional imaging study involving emotional unpredictability (Ran et al., 2016).

4.2. The co-activation network of emotional prediction

Our MACM analysis showed that significant co-activation for the DLPFC was observed in the inferior/middle and superior/medial frontal gyrus, inferior and superior parietal lobule, inferior/middle and superior temporal gyrus, inferior/middle occipital gyrus, anterior lobe, insula, fusiform gyrus, cingulate gyrus, postcentral gyrus, thalamus, caudate, lentiform nucleus, precuneus, and culmen. Interestingly, a similar network of coactivation was observed for the VLPFC and OFC. In particular, the identified networks of coactivation were largely overlapping, mostly involving the same brain areas. These areas of coactivation might show a co-activation network related to emotional prediction.

The DLPFC, VLPFC and OFC might be considered as core areas in the coactivation network of emotional prediction. The DLPFC has been shown to be associated with working memory and reward processing (D'Esposito, Postle, & Rypma, 2000; Haber & Knutson, 2010), also its role in prediction processing has been documented (Ran, Chen, Cao, & Zhang, 2016b). It is known that there is no direct anatomical connection between the DLPFC and the amygdala (Ray & Zald, 2011). Therefore, the DLPFC is not strongly associated with emotional prediction processing, it might exert a more indirect influence over areas of emotional prediction generation by its projections to the brain areas involved in emotion regulation, such as the parietal associative areas and cingulate gyrus (Cieslik et al., 2013; Koechlin, Ody, & Kounelher, 2003; Ray & Zald, 2011).

There is evidence that the VLPFC plays a critical role in generating emotional prediction (Nitschke et al., 2006). Unlike the DLPFC, the VLPFC is thought to possess direct efferent anatomical connections to the amygdala (Ray & Zald, 2011). Furthermore, this area is anatomically connected to the superior temporal gyrus (Ongür, Ferry, & Price, 2003), which computes higher-order multi-modal integration and also influences amygdala activity (Müller, Cieslik, Turetsky, & Eickhoff, 2012). Recently, a high-quality meta-analysis research has concluded that the VLPFC is in an ideal position to integrate computations from various prefrontal cortices, as it is associated with the medial prefrontal stream and the orbital prefrontal stream (Kohn et al., 2014).

It has previously been shown that the OFC is a multimodal association-processing area (e.g. Rolls, 2004), suggesting that this area is well suited for generating emotional prediction (Kveraga et al., 2007). Anatomically, the OFC is known to be connected with the temporal gyrus cortex and has reciprocal connections with the thalamus (Kringelbach & Rolls, 2004; Ongür & Price, 2000). According to a top-down facilitation model (Bar, 2003), a low spatial frequency representation of a input image is projected to the OFC from early visual or subcortical areas. The OFC then uses this low spatial frequency information to generate a set of predictions. Although the current study explored the brain areas associating emotional prediction, it was not optimal. It is nice to examine the moderating variables (e.g. gender, age and race) for the relationship between brain areas and emotional prediction in further research.

5. Conclusion

While a wealth of research has documented the neural correlates of emotional prediction (Barbalat, Bazargani, & Blakemore, 2013; Herwig et al., 2007; Nitschke et al., 2006), there has been no study to date that employs a meta-analytic approach to map the areas involved in emotional prediction. Our ALE analysis revealed significant convergent activations in the VLPFC, OFC, DLPFC, MPFC, PMC, MOG, ACC, amygdala, lingual gyrus, parahippocampal gyrus and cerebellum. Several prefrontal brain areas (VLPFC, OFC, DLPFC and MPFC) were proposed to play an important role in emotional prediction processing. For the MACM analysis, we found that the DLPFC, VLPFC and OFC were the core areas in the coactivation network of emotional prediction. Our findings contribute to a better understanding of the neural mechanisms of emotional prediction and the growing body of literature using the meta-analytic research techniques.

Funding

This research was supported by the Person of Outstanding Ability of China West Normal University (No. 17YC210), the Social Science Research "the 13 th Five-year Plan" Project for Sichuan Province in 2017 year (No. SC17C057), the Social Science Research "the 13th Five-year Plan" Project for Nanchong in 2016 year (No. NC2016B128/NC16B128) and the Doctoral Initiating Scientific Research Fund of China West Normal University (No. 16E023).

Compliance with ethical standards

Conflict of interest

Guangming Ran declares that he has no conflict of interest.

Ethical approval

This article does not contain any studies with human participants or animals performed by any of the authors.

Informed consent

No informed consent was obtained because no human participants were included in this study.

References

Aupperle, R. L., Allard, C. B., Grimes, E. M., Simmons, A. N., Flagan, T., Behrooznia, M., et al. (2012). Dorsolateral prefrontal cortex activation during emotional anticipation and neuropsychological performance in posttraumatic stress disorder. *Archives of General Psychiatry, 69*(4), 360–371.

Bar, M. (2003). A cortical mechanism for triggering top-down facilitation in visual object recognition. *Journal of Cognitive Neuroscience, 15*(4), 600–609.

Barbalat, G., Bazargani, N., & Blakemore, S. J. (2013). The influence of prior expectations on emotional face perception in adolescence. *Cerebral Cortex, 23*(7), 1542–1551.

Bermpohl, F., Pascualleone, A., Amedi, A., Merabet, L. B., Fregni, F., Gaab, N., et al. (2006). Dissociable networks for the expectancy and perception of emotional stimuli in the human brain. *Neuroimage, 30*(2), 588–600.

Brühl, A. B., Viebke, M. C., Baumgartner, T., Kaffenberger, T., & Herwig, U. (2011). Neural correlates of personality dimensions and affective measures during the anticipation of emotional stimuli. *Brain Imaging and Behavior, 5*(2), 86–96.

Chen, X., Ran, G., Zhang, Q., & Hu, T. (2015). Unconscious attention modulates the silencing effect of top-down predictions. *Consciousness and Cognition, 34*(5), 63–72.

Cieslik, E. C., Zilles, K., Caspers, S., Roski, C., Kellermann, T. S., Jakobs, O., et al. (2013). Is there "One" DLPFC in cognitive action control? Evidence for heterogeneity from co-activation-based parcellation. *Cerebral Cortex, 23*(11), 2677–2689.

Clauss, J. A., Cowan, R. L., & Blackford, J. U. (2011). Expectation and temperament moderate amygdala and dorsal anterior cingulate cortex responses to fear faces. *Cognitive, Affective, & Behavioral Neuroscience, 11*(1), 13–21.

Cromheeke, S., & Mueller, S. C. (2014). Probing emotional influences on cognitive control: An ALE meta-analysis of cognition emotion interactions. *Brain Structure and Function, 219*(3), 995–1008.

D'Esposito, M., Postle, B. R., & Rypma, B. (2000). Prefrontal cortical contributions to working memory: Evidence from event-related fMRI studies. *Experimental Brain Research, 133*(1), 3–11.

Dzafic, I., Martin, A. K., Hocking, J., Mowry, B., & Burianová, H. (2016). Dynamic emotion perception and prior expectancy. *Neuropsychologia, 86*, 131–140.

Eickhoff, S. B., Bzdok, D., Laird, A. R., Roski, C., Caspers, S., Zilles, K., et al. (2011). Co-activation patterns distinguish cortical modules, their connectivity and functional differentiation. *Neuroimage, 57*(3), 938–949.

Eickhoff, S. B., Laird, A. R., Grefkes, C., Wang, L. E., Zilles, K., & Fox, P. T. (2009). Coordinate-based activation likelihood estimation meta-analysis of neuroimaging data: A random-effects approach based on empirical estimates of spatial uncertainty. *Human Brain Mapping, 30*(9), 2907–2926.

Eysenck, M. W. (1997). Anxiety and cognition: A unified theory. *Essays in Cognitive Psychology*.

Feng, C., Luo, Y. J., & Krueger, F. (2015). Neural signatures of fairness-related normative decision making in the ultimatum game: A coordinate-based meta-analysis. *Human Brain Mapping, 36*(2), 591–602.

Friston, K. (2005). A theory of cortical responses. *Philosophical Transactions of the Royal Society B: Biological Sciences, 360*(1456), 815–836.

Friston, K. (2009). The free-energy principle: A rough guide to the brain? *Trends in Cognitive Sciences, 13*(7), 293–301.

Greenberg, T., Carlson, J. M., Rubin, D., Cha, J., & Mujica-Parodi, L. (2014). Anticipation of high arousal aversive and positive movie clips engages common and distinct neural substrates. *Social Cognitive & Affective Neuroscience, 10*(4), 605–611.

Grillon, C. (2008). Models and mechanisms of anxiety: Evidence from startle studies. *Psychopharmacology (Berl), 199*(3), 421–437.

Haber, S. N., & Knutson, B. (2010). The reward circuit: Linking primate anatomy and human imaging. *Neuropsychopharmacology Official Publication of the American College of Neuropsychopharmacology, 35*(1), 4–26.

Hamann, S. B., & Kilts, C. D. (2002). Ecstasy and agony: Activation of the human amygdala in positive and negative emotion. *Psychological Science, 13*(2), 135–141.

Herwig, U., Abler, B., Walter, H., & Erk, S. (2007a). Expecting unpleasant stimuli – An fMRI study. *Psychiatry Research Neuroimaging, 154*(1), 1–12.

Herwig, U., Baumgartner, T., Kaffenberger, T., Brühl, A., Kottlow, M., Schreiter-Gasser, U., et al. (2007b). Modulation of anticipatory emotion and perception processing by cognitive control. *Neuroimage, 37*(2), 652–662.

Herwig, U., Kaffenberger, T., Baumgartner, T., & Jäncke, L. (2007c). Neural correlates of a 'pessimistic' attitude when anticipating events of unknown emotional valence. *Neuroimage, 34*(2), 848–858.

Koechlin, E., Ody, C., & Kounelher, F. (2003). The architecture of cognitive control in the human prefrontal cortex. *Science, 302*(5648), 1181–1185.

Kohn, N., Eickhoff, S. B., Scheller, M., Laird, A. R., Fox, P. T., & Habel, U. (2014). Neural network of cognitive emotion regulation – An ALE meta-analysis and MACM analysis. *Neuroimage, 87*(2), 345–355.

Kok, P., Jehee, J. F., & de Lange, F. P. (2012). Less is more: Expectation sharpens representations in the primary visual cortex. *Neuron, 75*(2), 265–270.

Kringelbach, M. L., & Rolls, E. T. (2004). The functional neuroanatomy of the human orbitofrontal cortex: Evidence from neuroimaging and neuropsychology. *Progress in Neurobiology, 72*(5), 341–372.

Kveraga, K., Ghuman, A. S., & Bar, M. (2007). Top-down predictions in the cognitive brain. *Brain and Cognition, 65*(2), 145–168.

Laird, A. R., Eickhoff, S. B., Rottschy, C., Bzdok, D., Ray, K. L., & Fox, P. T. (2013). Networks of task co-activations. *Neuroimage, 80*(1), 505–514.

Laird, A. R., Fox, P. M., Price, C. J., Glahn, D. C., Uecker, A. M., Lancaster, J. L., et al. (2005). ALE meta-analysis: Controlling the false discovery rate and performing statistical contrasts. *Human Brain Mapping, 25*(1), 155–164.

Lanteaume, L., Khalfa, S., Régis, J., Marquis, P., Chauvel, P., & Bartolomei, F. (2007). Emotion induction after direct intracerebral stimulations of human amygdala. *Cerebral Cortex, 17*(6), 1307–1313.

Lin, H., Gao, H., Ye, Z., Wang, P., Tao, L., Ke, X., et al. (2012). Expectation enhances event-related responses to affective stimuli. *Neuroscience Letters, 522*(2), 123–127.

Lutz, J., Herwig, U., Opialla, S., Hittmeyer, A., Rufer, M., & Grosse, H. M. (2013). Mindfulness and emotion regulation – An fMRI study. *Social Cognitive and Affective Neuroscience, 9*(6), 776–785.

Müller, V. I., Cieslik, E. C., Turetsky, B. I., & Eickhoff, S. B. (2012). Crossmodal interactions in audiovisual emotion processing. *Neuroimage, 60*(1), 553–561.

Nitschke, J. B., Sarinopoulos, I., Mackiewicz, K. L., Schaefer, H. S., & Davidson, R. J. (2006). Functional neuroanatomy of aversion and its anticipation. *Neuroimage, 29*(1), 106–116.

Ongür, D., Ferry, A. T., & Price, J. L. (2003). Architectonic subdivision of the human orbital and medial prefrontal cortex. *Journal of Comparative Neurology, 460*(3),

425–449.
Ongür, D., & Price, J. L. (2000). The organization of networks within the orbital and medial prefrontal cortex of rats, monkeys and humans. *Cerebral Cortex, 10*(3), 206–219.
Onoda, K., Okamoto, Y., Toki, S., Ueda, K., Shishida, K., Kinoshita, A., et al. (2008). Anterior cingulate cortex modulates preparatory activation during certain anticipation of negative picture. *Neuropsychologia, 46*(1), 102–110.
Palermo, S., Benedetti, F., Costa, T., & Amanzio, M. (2015). Pain anticipation: An activation likelihood estimation meta-analysis of brain imaging studies. *Human Brain Mapping, 36*(5), 1648–1661.
Peng, M., De, B. A., Yuan, L., & Zhou, R. (2012). The processing of anticipated and unanticipated fearful faces: An ERP study. *Neuroscience Letters, 526*(2), 85–90.
Ran, G., Chen, X., Cao, X., & Zhang, Q. (2016b). Prediction and unconscious attention operate synergistically to facilitate stimulus processing: An fMRI study. *Consciousness and Cognition, 44*, 41–50.
Ran, G. M., Chen, X., Pan, Y. G., Hu, T. Q., & Ma, J. (2014). Effects of anticipation on perception of facial expressions. *Perceptual and Motor Skills, 118*(1), 195–209.
Ran, G., Chen, X., Zhang, Q., Ma, Y., & Zhang, X. (2016a). Attention Modulates Neural Responses to Unpredictable Emotional Faces in Dorsolateral Prefrontal Cortex. *Frontiers in Human Neuroscience, 10*.
Ray, R., & Zald, D. H. (2011). Anatomical insights into the interaction of emotion and cognition in the prefrontal cortex. *Neuroscience & Biobehavioral Reviews, 36*(1), 479–501.
Robinson, J. L., Laird, A. R., Glahn, D. C., Lovallo, W. R., & Fox, P. T. (2010). Metaanalytic connectivity modeling: Delineating the functional connectivity of the human amygdala. *Human Brain Mapping, 31*(2), 173–184.
Rolls, E. T. (2004). The functions of the orbitofrontal cortex. *Brain and Cognition, 55*(1), 11–29.
Sarinopoulos, I., Grupe, D. W., Mackiewicz, K. L., Herrington, J. D., Lor, M., Steege, E. E., et al. (2010). Uncertainty during anticipation modulates neural responses to aversion in human insula and amygdala. *Cerebral Cortex, 20*(4), 929–940.
Schienle, A., Köchel, A., Ebner, F., Reishofer, G., & Schäfer, A. (2010). Neural correlates of intolerance of uncertainty. *Neuroscience Letters, 479*(3), 272–276.
Schlund, M. W., Verduzco, G., Cataldo, M. F., & Hoehnsaric, R. (2012). Generalized anxiety modulates frontal and limbic activation in major depression. *Behavioral and Brain Functions, 8*(1), 1–5.
Simmons, A. N., Flagan, T. M., Wittmann, M., Strigo, I. A., Matthews, S. C., Donovan, H., et al. (2013). The effects of temporal unpredictability in anticipation of negative events in combat veterans with PTSD. *Journal of Affective Disorders, 146*(3), 426–432.
Simmons, A., Matthews, S. C., Stein, M. B., & Paulus, M. P. (2004). Anticipation of emotionally aversive visual stimuli activates right insula. *NeuroReport, 15*(14), 2261–2265.
Simmons, A. N., Stein, M. B., Strigo, I. A., Arce, E., Hitchcock, C., & Paulus, M. P. (2011). Anxiety positive subjects show altered processing in the anterior insula during anticipation of negative stimuli. *Human Brain Mapping, 32*(11), 1836–1846.
Simmons, A., Strigo, I., Matthews, S. C., Paulus, M. P., & Stein, M. B. (2006). Anticipation of aversive visual stimuli is associated with increased insula activation in anxiety-prone subjects. *Biological Psychiatry, 60*(4), 402–409.
Ueda, K., Okamoto, Y., Okada, G., Yamashita, H., Hori, T., & Yamawaki, S. (2003). Brain activity during expectancy of emotional stimuli: An fMRI study. *NeuroReport, 14*(1), 51–55.